Food Chemistry: X 20 (2023) 100963

Contents lists available at ScienceDirect

Food Chemistry: X

journal homepage: www.sciencedirect.com/journal/food-chemistry-x

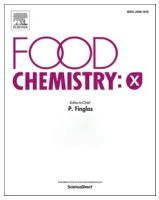

The roles of novel chitooligosaccharide-peanut oligopeptide carbon dots in improving the flavor quality of Chinese cabbage

Bosi Lu [a], Xiaojuan Chen [a,b], Xin Ouyang [a], Zhiming Li [a], Xujian Yang [a], Zaid Khan [a], Songpo Duan [a], Hong Shen [a,*]

[a] College of Natural Resources and Environment, South China Agricultural University, Guangzhou, Guangdong 510642, China
[b] College of Agriculture, Guangxi University, Nanning 530004, China

ARTICLE INFO

Keywords:
Chitooligosaccharide-peanut oligopeptide-carbon dots
Fluorescent properties
Chinese cabbage
Flavor quality
Retain freshness

ABSTRACT

Carbon dots (CDs), a novel type of nanomaterial, play crucial roles in the agriculture field. However, it remains unclear their impacts on the flavor quality of vegetables. The present study synthesized a novel chitooligosaccharide-peanut oligopeptide-carbon dots (COS-POP-CDs) material through the chitooligosaccharide (COS) and peanut oligopeptide (POP) high temperature Maillard reactions and studied its effect on the flavor quality of Chinese cabbage (Choy sum). Results indicated that COS-POP-CDs emit blue visible light that readily absorbed by chloroplasts, while also demonstrating some degree of antibacterial and antioxidant activities. After transplanting of Choy sum, foliar spraying 0.12 mg/mL COS-POP-CDs twice can increase the content of soluble proteins, Vitamin C, and enhance the strawberry and spicy flavors of Choy Sum. After harvest of Choy Sum, foliar spraying 0.12 mg/mL COS-POP-CDs once can slow down the spoilage. These results suggest that COS-POP-CDs have significant potential to improve crop quality.

1. Introduction

Vegetables have been an indispensable green food on people's tables since ancient times. The International Cancer Conference reported that diets including vegetables can prevent the occurrence of various common diseases, and their anticancer effects are even better (Slavin, & Lloyd, 2012). Among them, cruciferous vegetables have multiple nutrients required by humans, they are rich in β-carotene, glucosinolates, vitamins, minerals, flavonoids, anthocyanins, dietary fiber, and especially a sulfur compound called mustard oil glycoside. The isothiocyanates formed by the degradation of this substance, perform a variety of biological activities such as antioxidation, tumor inhibition, and immunity regulation (Lucarini, Micheli, Di Cesare Mannelli, & Ghelardini, 2022).

However, the excessive use of chemical fertilizers has directly or indirectly led to soil problems such as acidification, compaction, and salinization. The decrease in the replanting index has led to a low photosynthetic efficiency of shallow-rooted crops. Additionally, the delicate nature of cruciferous vegetables makes them vulnerable to environmental damage. In the southern part of China, excessive rainfall and persistent high temperatures make the surface of vegetables a conducive breeding ground for spoilage microbes, subsequently affecting the biosynthesis of primary and secondary metabolites that drive the production of flavor quality. These factors ultimately lead to a reduction in crop yield and shorter shelf life. Given the above-mentioned issues, new strategies to enhance the photosynthetic efficiency and extend the freshness of cruciferous vegetables hold significant practical importance.

Carbon dots (CDs) are a type of novel nanomaterial with dimensions less than 10 nm. They possess a core–shell structure, with active functional groups such as carboxyl, hydroxyl, and amino groups adorning the surface of their amorphous carbon skeletons. The abundant oxygen-containing groups on the surface provide them with excellent water solubility, photoluminescence, antioxidant activity, and antibacterial properties (Muthamma, Sunil, & Shetty, 2021). The synthesis methods for CDs can be broadly classified into two categories: 'top-down' and 'bottom-up'. The 'top-down' approach for preparing CDs involves breaking down large molecular materials through methods such as electro-oxidation and laser ablation. However, the process requires a long time, and the cost is relatively high. The 'bottom-up' synthesis from natural biomaterials is achieved through the condensation-linkage-carbonization of small molecule precursors. This method, which

* Corresponding author.
E-mail address: hshen@scau.edu.cn (H. Shen).

https://doi.org/10.1016/j.fochx.2023.100963
Received 15 August 2023; Received in revised form 11 October 2023; Accepted 23 October 2023
Available online 30 October 2023

includes microwave-assisted, electrochemical treatment, and hydrothermal methods, is characterized by its low cost, simple procedure, and high reaction efficiency. In fact, almost all carbon-containing materials can serve as sources for carbon dot synthesis (Đorđević et al., 2022). Currently, CDs have been extensively applied in fields such as agricultural production, fluorescence imaging, drug delivery, and chemical sensing (Mao et al., 2019).

In the agricultural food sector, commonly used nanomaterials include metal oxide nanoparticles, silicate nanoparticles, luminescent nanomaterials, and organic–inorganic composites, however, these nanomaterials pose certain biotoxicity and ecological risks (Farooq et al., 2022). Compared with other nanomaterials, the CDs synthesized from pure plants possess the characteristic of being non-biotoxic (Liu et al., 2022). Biological photosynthesis is the source of all things, yet only 10 % of sunlight is captured and utilized by plants. When the fluorescence emission spectrum of CDs overlaps significantly with the absorption spectrum of chloroplasts, these chloroplasts can partially absorb the excitation energy of CDs (Li et al., 2018). The photosynthetic pigments and electron transfer system on the thylakoid membrane of plant chloroplasts (Shimakawa, 2023) release oxygen and generate NADPH after being excited by light, simultaneously promoting photosynthetic phosphorylation to generate ATP, supplying a pathway for CO_2 fixation. Previous research shows that CDs can easily penetrate cell walls and accumulate in leaf veins act as both electron donors and acceptors, accelerating the electron transfer rate in photosystem II (Li et al., 2017; He et al., 2020). Therefore, the nanoscale properties and photoluminescent characteristics of CDs supply a theoretical basis for their application of enhancing plant photosynthesis.

Chitooligosaccharides (COS), the only oligosaccharides with a positive charge in nature, research proved that the chitosan's antibacterial activity depends on its sugar chain length, the smaller molecular weight presents higher fluidity and a stronger antibacterial ability, a feature that can be attributed to the nitrogenous groups on their carbon chains (Ailincai et al., 2022). Peanut oligopeptide (POP) is extracted from peanut protein using enzymolysis techniques, it is rich in lysine, glutamic acid, cysteine, and aspartic acid. Glutamic acid's -SH can neutralize free radicals produced by lipid oxidation, the S—S structure formed by cysteine and the cysteine residue in glutathione can capture free radicals and chelate metal ions, inhibiting oxidative stress responses in both animals and plants, thereby reducing cellular oxidative damage (Yu, & Klionsky, 2022). In the agriculture food field, POP is often used as nutritional supplements in animal feed, but its use as a raw material for novel CDs synthesis is rarely reported.

Maillard reaction (MR), also known as the carbonyl–amine reaction, produces brown or deep brown melanoidin substances when reducing carbonyl compounds and amino compounds (proteins, peptides, and amino acids) when reacting under heating conditions (Wang et al., 2017). The skeleton structure of melanoidin's is mainly composed of unsaturated carbonyl compounds of sugars, with free oligopeptides or amino acids cross-linked as side chains. Researchers first discovered foodborne fluorescent CDs in 2012 and confirmed that CDs formed at higher temperatures are smaller than those formed at lower temperatures (Sk et al., 2012). Previous research shows that the formation of foodborne CDs is closely linked to the Maillard reaction. Evidence shows that the colored substances, Amadori compounds, produced at the early stage of the Maillard reaction do not possess fluorescent characteristics. During the intermediate stage of the Maillard reaction, multi-carbon compounds such as aldehydes, ketones, and heterocyclic compounds are formed, which undergo fragmentation reactions, followed by rearrangement, condensation, and isomerization. In the later stage of the Maillard reaction, these compounds further condense to form melanoidins, and in this process, fluorescent CDs are generated. Although, the specific mechanism for the formation of food-derived CDs is not yet clear, but some scholars have already conducted partial research on the application of food-derived carbon dots. Wei et al. (2014) prepared MRPs using glucose and amino acids, then carbonized them with microwave to gain small-size CDs. Fu et al. (2022) used chitosan as a precursor to synthesize multifunctional fluorescent CDs. A bio-nanocomposite film based on Gelatin/Chitosan incorporated with CDs was developed. It was found that the prepared bio-nanocomposite film not only can improve the quality and shelf life of fish meat, but also can indicate the freshness of the fish meat.

The objective of this study is to develop a novel CDs material by combining COS, which possesses high antibacterial activity, with POP, known for their high antioxidant activity, through the Maillard reaction. The results of our work revealed that COS-POP-CDs were successfully synthesized and exhibited excellent fluorescent properties and nanoscale dimensions. COS-POP-CDs enhance the flavor quality of Choy sum by improving its photosynthesis and enhanced the crop's antioxidant enzyme system activities. Furthermore, they alleviate the damage to the chloroplasts of Choy sum, this intervention aids in delaying cell aging and preserving the content of essential nutrients after harvest.

2. Materials and methods

2.1. Materials

Chitooligosaccharides (COS, MW $\leq$ 2000) of 2 % (w/v), Peanut oligopeptide solution (30 g/L), *Escherichia coli* (ATCC 25922) and *Staphylococcus aureus* (ATCC 43300) were provided by the Rhizosphere Regulation Laboratory of South China Agricultural University. Other reagents were all analytical grade and provided by Guangzhou Chemical Reagent Factory.

2.2. Preparation process of CDs

COS and POP solutions were mixed in a 3:1 (w/w) ratio and transferred to a Teflon-lined stainless-steel chamber. The pH was adjusted to 7.0, and the reaction was conducted at (67 °C, 200 r/min, and 32 min). Subsequently, the temperature was rapidly increased to 180 °C, and the reaction was conducted at 180 r/min for 6 h. After the reaction was completed, the mixture was cooled to room temperature. The resulting sample was centrifuged at 10,000 r/min at 4 °C for 10 min, and the supernatant was passed through a 0.22 μm filter membrane. The obtained COS-POP-CDs were then dialyzed using dialysis bag with a cutoff molecular weight of 7000 Daltons for 60 h. The COS-POP-CDs were freeze-dried and stored at 4 °C for further use. COS-CDs and POP-CDs were directly prepared in Teflon stainless-steel chamber at 180 °C, reaction was conducted at 180 r/min for 6 h, and the rest of steps were the same as COS-POP-CDs.

2.3. Characterizations

Fourier transform infrared spectroscopy (FTIR) spectra of the COS-CDs, POP-CDs and COS-POP-CDs were recorded on a Bruker spectrophotometer (VERTEX 70, Germany) with a resolution of 4 cm^{-1}. A KBr disk containing 0.1 % finely ground COS-CDs, POP-CDs, and COS-POP-CDs were used for determination. An average of 16 scans ranging from 400 cm^{-1} to 4000 cm^{-1} were used. The absorption spectra in the range from 200 to 700 nm were measured using a UV–Vis spectrophotometer (PerkinElmer, Waltham, USA). The fluorescence spectra of the COS-POP-CDs were measured using a fluorescence spectrophotometer (FSP, FluoroMax-4, Horiba, USA). The morphological structure, nanoparticle size, and Zeta potential of the samples were analyzed using transmission electron microscopy (Thermo Scientific ESCALAB Xi, USA) operated at 300 kV and a Zeta potential and particle size analyzer (Zetasizer Nano ZS 90), the CDs materials were measured by an Escalab 250Xi X-ray photoelectron spectrometer (XPS, Thermo Scientific K-Alpha, USA), respectively.

2.4. In vitro antibacterial and antioxidant capacity

2.4.1. Antibacterial

E. coli and *S. aureus* were cultured in Luria-Bertani medium until the optical density (OD_{600}) ranged between 0.6 and 0.8. With 1 % (v/v) inoculate amount into a 250 mL Erlenmeyer flask containing 50 mL of Luria-Bertani liquid medium and further incubated at 37 ℃ and 180 r/min. Subsequently, different concentrations (0.05, 0.10, 0.20, 0.40 mg/mL) of COS-POP-CDs were added into the respective mediums. The OD_{600} of the medium was measured at hourly intervals.

CDs solutions of varying concentrations (0.20, 0.40, 0.60, 0.80 mg/mL) were prepared. Filter paper circles of 0.5 cm diameter, created using a puncher, were immersed in the CDs solution for 5 min. After 12 h, the diameters of the inhibition zones created by these diverse concentrations of CDs against *E. coli* and *S. aureus* were compared. The morphologies of the bacterial were examined using Scanning electron microscopy (SEM, EVO MA 15, Carl Zeiss, Germany).

2.4.2. DPPH radical scavenging activity

The DPPH radical scavenging rate based on a previously published method reference with slightly modification (Shaik et al., 2022): A diluted sample solution (1 mL) was mixed with 2 mL of 0.2 mmol/L DPPH-ethanol solution. After thorough mixing, the mixture was kept in the dark for 30 min, and the absorbance at 517 nm was measured and recorded as A_1. Similarly, the absorbance of a blank sample (pure water) with an identical measure procedure was recorded as A_0. The DPPH radical scavenging rate was calculated using the following formula.

$$\text{Scavenging rate}\,(\%) = \frac{A_0 - A_1}{A_0} \times 100\% \quad (1)$$

2.4.3. Superoxide anion radical scavenging rate

The superoxide anion radical scavenging rate was determined as follows (Milanović et al., 2023): Tris-HCl buffer solution (pH 8.2) was prepared, and 5 mL of the buffer solution was mixed with 4.7 mL of pure water. The mixture was equilibrated in a water bath at 25 °C for 20 min, followed by the addition of 0.3 mL of preheated (25 ℃) pyrogallol (3 mmol/L) solution. After thorough shaking, the absorbance was measured at 325 nm. The reaction time was 3 min, and the absorbance was recorded 6 times every 30 s. The average of the differences between each successive measurement was noted as A_0, the distilled water was replated sample solution recorded as A_1. The superoxide anion radical scavenging rate was calculated using Eq. (1).

2.4.4. ABTS radical cation scavenging activity

The determination of anti-lipid peroxidation capacity was performed as follows (Xu et al., 2022): The sample solution was diluted to a certain multiple, and 1 g of edible peanut oil was mixed with 200 mg of the diluted sample solution and 5 mL of 2.8 g/L TBA (thiobarbituric acid). The mixture was reacted in a constant temperature oven at 90 °C for 6 h. After cooling, 5 mL of 100 g/L TCA and 2 mL of $CHCl_3$ were added, followed by thorough shaking and a 10 min rest. The supernatant was collected, and the absorbance was recorded as A_1 at 532 nm. Distilled water was used as a substitute for the sample and subjected to the same oven treatment as the control group, The absorbance was recorded as A_0. The ABTS radical scavenging was calculated using Eq. (1).

2.4.5. Hydroxyl radical scavenging activity

Based on a previously published method reference with slightly modification (Chen, Huang, Yang, & Hou, 2019). Diluted solutions of peanut Oligopeptides liquid were prepared. One milliliter of the sample dilution was mixed with 1 mL of salicylic acid–ethanol solution, 1 mL of ferrous sulfate solution (9 mmol/L)、1 mL H_2O_2 (0.30 %, w/w), This mixture was then allowed to rest at a constant temperature of 37 °C for 30 min. Subsequently, the absorbance of the resulting solution at 510 nm was recorded, and this reading was appointed as A_1. For the control measurement, labeled as A_0, the distilled water in the original mix was replaced with the sample solution. Furthermore, an added measurement, A_2, was taken, wherein the procedure was replicated except for omitting the addition of H_2O_2.

$$\text{Scavenging rate}\,(\%) = 1 - \frac{A_1 - A_2}{A_0} \times 100\% \quad (2)$$

2.5. Pot experiments of CDs on Choy sum

'Oil Qing Choy sum' was selected as the experimental material (provided by the Vegetable Research Institute of Guangdong Academy of Agricultural Sciences). Seeds were sterilized with 5 % (w/w) hydrogen peroxide and were placed into the substrate on seedling trays under dark conditions for germination. Then, the seedlings were watered regularly. After 3 d, the visible germinated seedlings were transferred to a growth chamber with illumination. When the Choy sum plants reached the stage of four true leaves, they were transplanted into plastic pots with dimensions of 15 cm (height), 10 cm (top width), and 6 cm (bottom width). Each pot was filled with 500 g of a soil mixture consisting of arable soil and substrate (4:1) collected from the greenhouse of the College of Natural Resources and Environment, South China Agricultural University. A basal fertilizer (15–15–15) was applied at 0.4 g. Different concentrations (0.04–0.20 mg/mL) of CDs were sprayed after transplanting 10 d and 20 d, a total of treatment 2 times. Samples were taken every 4 d intervals after each treatment, as well as on the 28 d to determine the expression of antioxidant enzyme-related genes.

The superoxide anion in Choy sum leaves was measured using Nitrotetrazolium Blue chloride (NBT). A 0.5 mg/mL NBT reagent was prepared, and the plant samples were immersed in it, then stained for 3 h at 28 °C in darkness. After the staining process was completed, the leaves were transferred to an 80 % (v/v) ethanol solution and boiled in a water bath for 10 min until all green color from the leaves was completely removed. Then, anhydrous ethanol was added, and the solution was stored in a 4 ℃ refrigerator for some time before observation.

The photosynthetic parameters, including net photosynthetic rate (Pn), transpiration rate (Tr), and stomatal conductance (Gs) of the third functional leaf (from top to bottom), were measured using a Li-6400XT portable photosynthesis system. The instrument condition was set to a light intensity of 1000 μmol/m^2·s and CO_2 concentration of 400 μmol/mol. Each treatment was replicated 4 times.

The chlorophyll content was determined as follows: 0.1 g of leaf sample was soaked in 20 mL of 95 % ethanol solution for 24 h in the dark. The absorbances at 664 nm, 648 nm, and 470 nm were measured, and the chlorophyll *a*, chlorophyll *b*, and carotenoid contents were calculated according to the following formula (Samynathan et al., 2023).

$$C_a = 13.36A_{664} - 5.19A_{648} \quad (3)$$

$$C_b = 27.43A_{664} - 8.12A_{648} \quad (4)$$

$$C_n = (1000A_{470} - 2.13C_a - 97.64C_b)/209 \quad (5)$$

where C_a is the content of chlorophyll *a* (mg/L), C_b is the content of chlorophyll *b* (mg/L), C_n is the carotenoid content (mg/L).

The determination of soluble proteins was performed using the Coomassie Brilliant Blue G-250 method. Two grams of fresh leaves were homogenized with 8 mL of water and the mixture was centrifuged at 10,000 r/min for 10 min. The supernatant was transferred to 10 mL volumetric flask and 5 mL of 0.1 % (w/w) Coomassie Brilliant Blue reagent was added. The absorbance at 595 nm was measured. Then, the soluble solid content was determined using a digital glucose meter (TD45, Guangzhou, China). Finally, the content of vitamin C was determined using molybdenum blue colorimetry (Laurentin & Edwards, 2003).

A 0.2 g sample of Choy sum was weighed and 1 mL of 50 mmol/L

phosphate buffer (pH 7.8) was added. The mixture was ground into a slurry under ice bath conditions. The volume was made up to 5 mL with buffer solution. The mixture was centrifuged at 10,000 rpm and 4 °C for 15 min. The supernatant was used for measuring antioxidant enzyme activity.

Malondialdehyde (MDA) was determined using the thiobarbituric (TAB) acid method, superoxide dismutase (SOD) was determined using the nitroblue tetrazolium (NBT) photochemical reduction method, and peroxidase (POD) was determined using the guaiacol colorimetric method. The catalase (CAT) activity was measured as the decline in absorbance at 240 nm due to the decrease of extinction of H_2O_2 (Li et al., 2023).

Plant total RNA extraction was conducted as follows: total RNA from Choy sum leaves was extracted and purified using a Spin Column Plant Total RNA Purification Kit (Sangon Biotech, China). An Aurora-800 ultramicro spectrophotometer (Aurora, HIPIE, China) was used for spectrophotometric analysis, and the concentration and purity of the extracted RNA were calculated from the A260/A280 ratio. RNA was transcribed into cDNA using a HiScript III 1st Strand cDNA Synthesis Kit with gDNA wiper (R323-01, Vazyme, China).

Detection of relevant genes was performed as follows: three antioxidant enzyme protein genes (*CsMn-SOD*, *Cs-POD*, *Cs-CAT*) were selected from the NCBI database. Synthesized by Wuhan Tianyi Huiyuan Biotechnology Co., Ltd., and then used for qRT-PCR. cDNAs were reverse transcribed as templates using an ABI7500 real-time fluorescent quantitative PCR instrument (ABI7500, Applied Biosystems, United States) and a fluorescent dye (Taq Pro Universal SYBR qPCR Master Mix, Vazyme, China) by qRT-PCR amplification. Three biological replicates were set up for each sample, and the internal reference gene was Actin. The $2^{-\Delta\Delta Ct}$ method was used to calculate the relative expression level of the genes.

2.6. After harvest of Choy sum

When harvesting choy sum, spray once with COS-POP-CDs of different concentrations (0.08–0.16 mg/mL). The spraying method is the same as the potted experiment, and the quality indicators of choy sum after harvesting were measured. Five grams of Choy sum sample were taken and transfered into a pH 7.0, 0.02 mol/L phosphate buffer solution. Then it was centrifuged at 8,000 r/min for 2 min at 4 °C. Using a sterile pipette, 1 mL of the supernatant was collected, then 9 mL of sterile buffer solution was added, these steps were repeated several times. After mixing thoroughly, a small amount was taken and placed on a sterile petri dish. The later was incubated at 36 °C for 48 h. Bacterial count was expressed in colony-forming units (CFUs). Water content was determined by drying method. Soluble protein, Vitamin C, MDA and antioxidant enzymes SOD, POD, CAT, the content of the determination method was the same as above.Volatile compounds in Choy sum leaves were extracted using the head-space solid-phase microextraction (HS-SPME) method and analyzed using a gas chromatograph coupled with a mass spectrometer (QP2010 ULTRA, Shimadzu Japan) (Cui et al., 2022).

2.7. Statistical analysis

Microsoft Excel 365 and SPSS 22.0 were used for data organization and analysis. Duncan's multiple comparison tests ($p < 0.05$) was used, and data denoted by the same letters indicate insignificant differences between the means. Origin 2022 software was used for plotting.

3. Results and discussion

3.1. FITR, UV–vis, Zeta potential and size, TEM observation

The COS and POP materials could be used to synthesize CDs, FTIR spectroscopic results revealed prominent absorption peaks at 3430 cm^{-1} and 1655 cm^{-1}, corresponding to OH– and C═O groups respectively, and absorption peaks at 1620 cm^{-1}, 1400 cm^{-1}, 1122 cm^{-1}, 620 cm^{-1} representing the stretching vibrations of C═C, COO–, C—O—C, S—S groups in the benzene ring (Cui et al., 2018). Not only that, COS-POP-CDs formed new N—H (3364 cm^{-1}) and O—C—O (930 cm^{-1}) functional groups (Fig. 1a). These findings were shown to indicate that an abundance of carbon–oxygen and carbon–nitrogen groups is possessed by COS-POP-CDs. These functional groups were likely to endow the CDs with good water solubility and some unique luminescent properties. The UV–Vis spectrum of COS-POP-CDs was revealed to absorption peaks at 265 nm and 300 nm, which could be attributed to the π-π* transitions of the C═C conjugated double bonds and the n-π* transitions of C═O signifying the formation of a graphite-like carbon structure at its core (Jang, et al., 2017).

The inset results were shown to the excitation at 360 nm wavelength, COS-CDs excited green fluorescence, POP-CDs excited blue-green fluorescence, COS-POP-CDs emitted shorter wavelength blue light (Fig. 1b). This has a higher overlap of absorption peaks with the blue light (430–450 nm) in chloroplasts (Jia, Li, & Wang, 2012). Zeta potential analysis of the three types of CDs showed that the COS-CDs, COS-POP-CDs, and POP-CDs had possessed zeta potential peaks near + 25 mV, +35 mV and + 40 mV, respectively. So, A positive charge at a high potential meant the stability and antibacterial ability of COS-POP-CDs and POP-CDs is superior to that of COS-CDs, indicating satisfactory dispersibility (Fig. 1c). The transmission electron microscopy TEM image clearly depicted that it is possible to get nano-sized particle from COS and POP, with uniformly dispersed spherical particle CDs visible across the field of vision. The particle size of COS-CDs, POP-CDs, and COS-POP-CDs was primarily found to be at 4.5 ± 1.2 nm, 5.4 ± 1.5 nm, and 3.2 ± 1.1 nm (Fig. 1d, 1e, 1f), respectively. While COS-POP-CDs had a smaller size, no significant difference between the three types of CDs was observed.

3.2. XPS, FSP, and in vitro antioxidant

Three different CDs samples were measured with XPS. The results shown that different types of CDs contained varying relative contents of C, N, and O elements. Among these, the nitrogen and oxygen content in COS-CDs were found to be 6.57 % and 30.83 %, respectively, while in POP-CDs, the nitrogen and oxygen content were recorded 10.09 % and 24.51 %, respectively. This suggested that there was a certain positive correlation between the newly formed carbon dots at high temperatures and the percentage content of each element in the raw materials (Leng et al., 2022). Interesting, COS-POP-CDs had the highest relative nitrogen content by 13.72 %, it could be indicated that more nitrogen-containing groups were formed in COS-POP-CDs (Fig. 2a).

The unique fluorescent properties were imparted to COS-POP-CDs by the nitrogen-containing functional groups such as amino and amide groups on the surface (Zhang et al., 2016). COS-POP-CDs high-resolution C 1 s peaks appeared at 288.2 eV, 286.3 eV, and 285.1 eV, corresponding to C—O/C—S, C═O/C═N, C—C bonds respectively (Koutamehr et al., 2023) (Fig. 2b). High-resolution O 1 s peaks emerged at 531.1 eV and 532.7 eV, corresponding to C═O/N═O and C—O/N—O bonds respectively (Fig. 2c), while high-resolution N 1 s peaks were appeared at 397.5 eV, 399.2 eV, 400.5 eV, and 401.4 eV, corresponding to C═N-C, C—N—C, C—N, and C═N bonds respectively (Wang et al., 2021) (Fig. 2d). When the surface of CDs was imbued with SP^2 and SP^3 hybridized carbon-derivative groups such as epoxy and carboxyl clusters, the defects instigated by these groups engendered fresh energy levels (Guo et al., 2022). These newly constituted energy levels can incite fluorescence across diverse wavelengths. The fluorescence emission of COS-POP-CDs from 290 nm to 430 nm was assessed by the FSP. As the emission wavelength extended, a gradual redshift of the emission peaks was seen, indicating the presence of multiple fluorescence excitation sites. Fluorescence intensity was initially increased and then decreased, and the highest emission of CDs was seen near at 370 nm. This further confirmed that COS-POP-CDs were a type of carbon dots

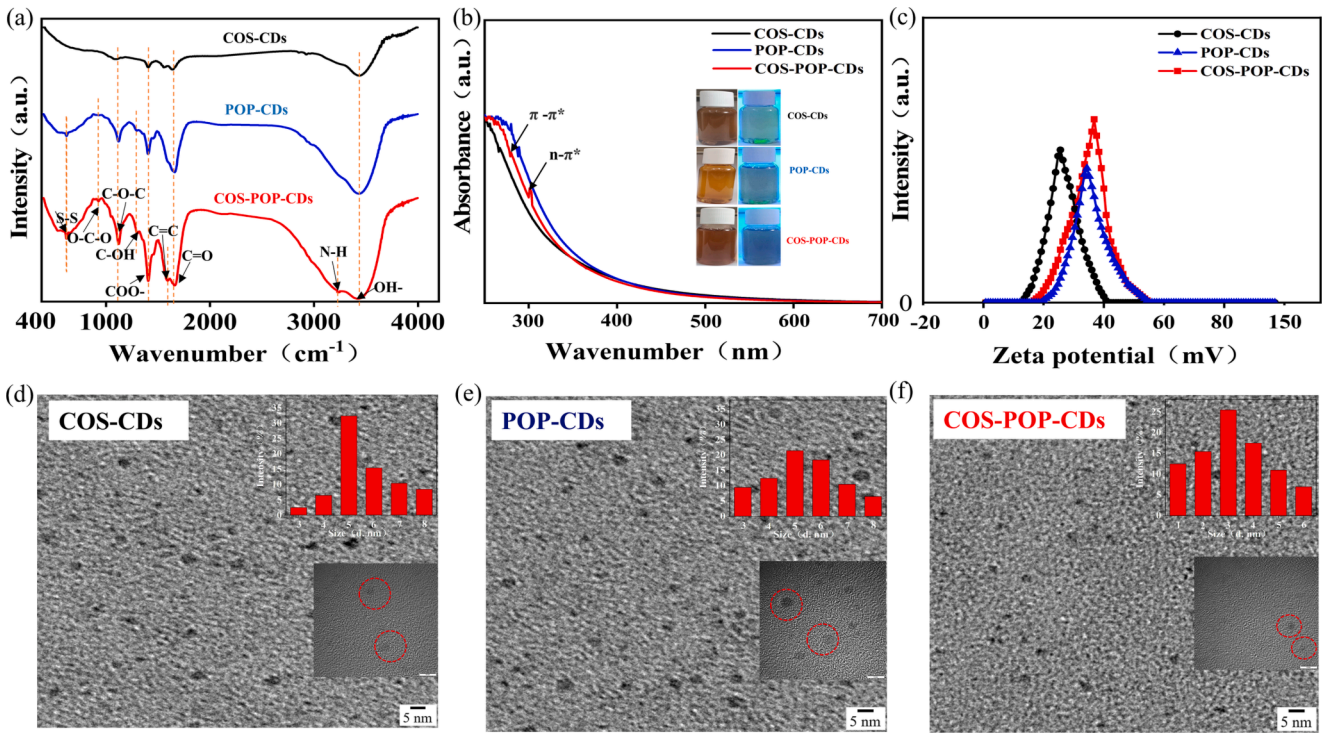

Fig. 1. FTIR spectra of COS-CDs, POP-CDs, and COS-POP-CDs (a). UV–vis absorption spectrum of COS-CDs, POP-CDs, and COS-POP-CDs, inset: the different CDs photoluminescence features (b). Zeta potential of COS-CDs, POP-CDs, and COS-POP-CDs (c). TEM and particle illustrations of COS-CDs (d), POP-CDs (e), and COS-POP-CDs (f), inset: average size of different CDs.

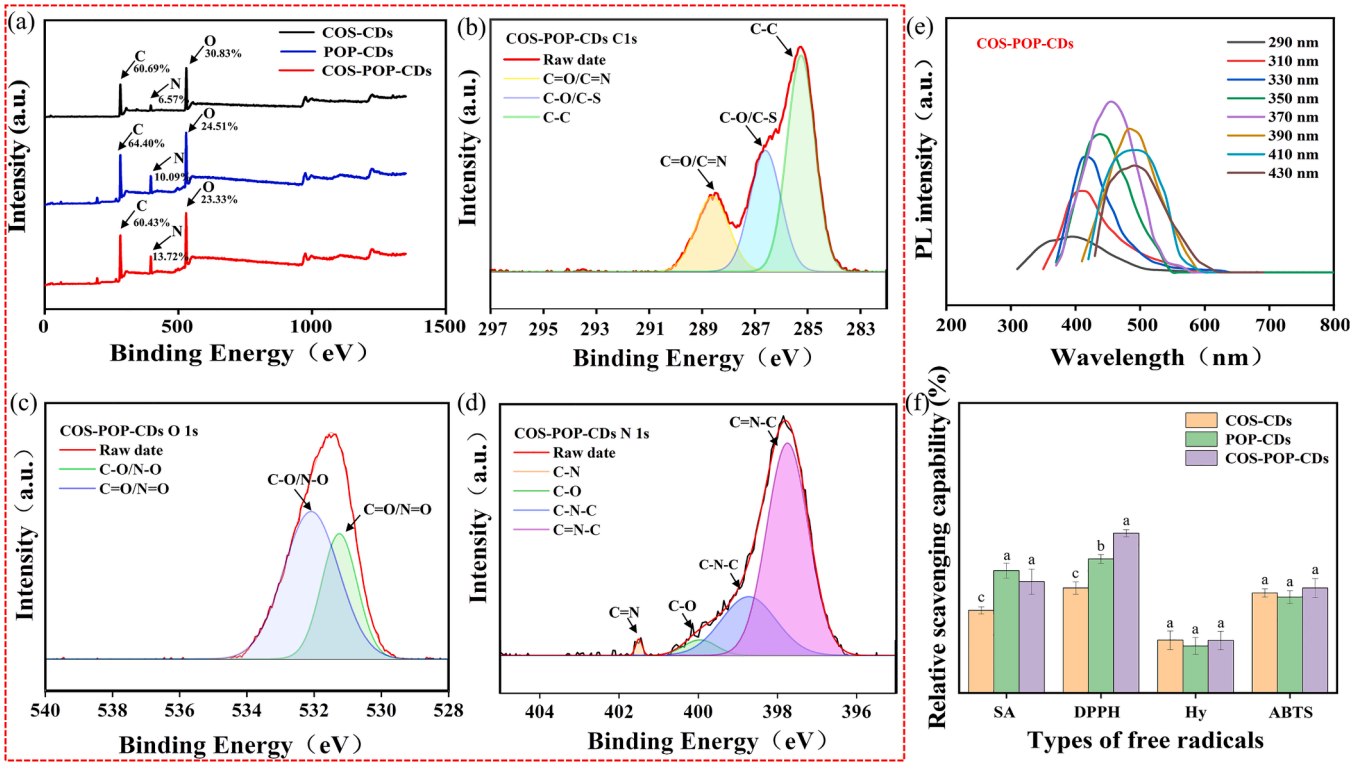

Fig. 2. XPS-Full spectra of COS-CDs, POP-CDs, and COS-POP-CDs (a). C1s of COS-POP-CDs (b). O1s of COS-POP-CDs (c). N1s of COS-POP-CDs (d). The emission spectrum from 290 nm to 430 nm of COS-POP-CDs (e). In vitro antioxidant activity of COS-CDs, POP-CDs, and COS-POPs-CDs (f). Different lowercase letters indicate significant differences among the treatments, based on the Duncan test ($p < 0.05$, n = 4).

that coordination well with plant photosynthesis (Fig. 2e). As shown in Fig. 2f, at the same concentration, the COS-CDs, POP-CDs, and COS-POP-CDs all exhibited commendable antioxidant abilities. Compared with COS-CDs and POP-CDs, COS-POP-CDs significantly performed more remarkably in terms of DPPH radical scavenging rate, but the differences in their hydroxyl radical and ABTS radical scavenging rates were not significant.

3.3. Antibacterial

Vegetables can absorb nutrients from environment to boost their immunity against adverse environmental stress (Khalid et al., 2023). Furthermore, the immune system of vegetables can be collapsed by rapid dehydration and root damage after harvesting, leading to the loss of cellular nutrients and a proliferation of decay-causing bacteria. Previous research has shown that the synthesis of CDs often keeps a part of the function from the raw Maillard reaction materials. Therefore, in this study, we assessed the effects of COS-POP-CDs on the growth of Gram-negative *E. coli* and Gram-positive *S. aureus*. The results showed that an appropriate concentration of COS-POP-CDs inhibits both types of bacteria, with a stronger inhibitory effect on *S. aureus* than on *E. coli*. Liquid culture test showed that the COS-POP-CDs demonstrate different inhibitory effects on *E. coli* and *S. aureus*. Specifically, when cultured for 4–6 h, a concentration of 0.20–0.40 mg/mL COS-POP-CDs showed a significant inhibitory effect on the bacterial concentration of *E. coli*, while a concentration range of 0.10–0.40 mg/mL COS-POP-CDs demonstrated an inhibitory effect on *S. aureus*.

Solid petri dish antibacterial experiments showed that the concentration of 0.20 mg/mL CDs almost didn't inhibit *E. coli* within 12 h, but progressively noticeable inhibition zones appeared with increasing concentration. On the other hand, the growth of *S. aureus* was significantly inhibited at concentrations of COS-POP-CDs between 0.20 and 0.80 mg/mL (Fig. 3a, 3c). This may be due to the abundant nitrogen-containing groups and very small size of COS-POP-CDs, the amino groups on their surface, which are positively charged, interact favorably with the negatively charged phosphate groups on the surface of Gram-positive bacteria, by electrostatic interaction disrupts the bacterial cell membrane, while also promoting the intracellular generation of ROS, so accelerating bacterial apoptosis (Ke et al., 2022). *E. coli* and *S. aureus* were observed by scanning electron microscope, COS-POP-CDs have distinct mechanisms of cell destruction for Gram-negative and Gram-positive bacteria. COS-POP-CDs can cause *E. coli* bacteria expand, shrink, and lose their activity, they can rupture *S. aureus* cells from the central depression, leading to their death (Fig. 3b, 3d), which concurred with the aforementioned results. In summary, COS-POP-CDs have satisfactory and substantial in vitro antibacterial capability even in low concentrations.

3.4. Cos-pop-cds on the growth of Choy sum

Aside from soilless cultivation, most agricultural planting primarily takes place in greenhouses or farmland. Previous research showed CDs can enter leaf cells through stomatal apertures on the leaf surface and be transported to other organs via the vascular system (Gao et al., 2023). Therefore, we conducted a pot experiment, in which different concentrations of COS-POP-CDs were sprayed on Choy sum to assess their influence on photosynthesis and growth, aiming to explore CDs potential application value in agricultural vegetable foods. As shown in Fig. 4a, compared with the CK treatment, leaf growth in Choy sum after transplanting 14 d and 28 d was promoted by spraying COS-POP-CDs, among these, the Choy sum treated with CD-1, CD-2 and CD-3 exhibited better growth and the leaves presented a deeper green color. The CD-2 treatment increases the fresh weight of Choy sum by 16.7 %-21.6 % and enhances its leaf SPAD value (Fig. 4b).

In comparison with the control treatment, the appropriate concentration of COS-POP-CDs used in the experiment had a significant influence on the contents of Vitamin C and soluble protein. As seen in Fig. 4c, CD-2 treatment had improved choy sum Vitamin C, soluble protein by 11.7 %, 13.9 %, respectively. After 14, 20, and 28 d of transplanting Choy sum, CD-2 treatment increased the net photosynthetic rate by 40.9 %, the transpiration rate by 15.4 %, and the stomatal conductance by 12 % (Fig. 4d, 4e, 4f). The accumulation of photosynthetic products in Choy sum is benefited by an increase in photosynthetic efficiency parameters. During plant photosynthesis, chloroplasts produce various ROS that can damage the photosystem, leading to breakdown of chlorophyll. After 28 d of transplantation, compared with the CK treatment, spraying COS-POP-CDs at concentrations 0.12 mg/mL significantly improved the content of chlorophyll-a and chlorophyll-b in Choy sum leaves, but hadn't significantly on the carotenoid content (Fig. 4g). This result has shown that CDs can even penetrate the cell wall and enter the cell to remove various free radicals (Ezati et al., 2022). Therefore, the results obtained could therefore be attributed to several combined factors. COS-

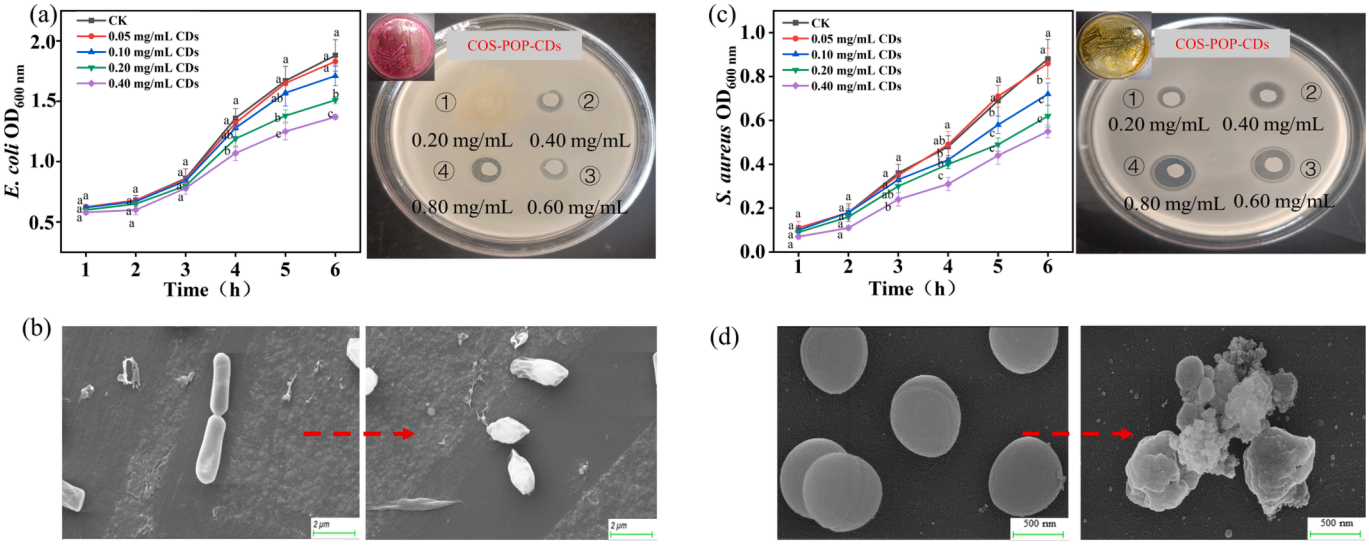

Fig. 3. Different concentrations of COS-POP-CDs growth inhibitory of *E. coli* in liquid and solid medium (a). Scanning electron microscope morphology of *E. coli* (b). Different concentrations of CDs growth inhibitory of *S. aureus* in liquid and solid medium (c). Scanning electron microscope morphology of *S. aureus* (d). Different lowercase letters indicate significant differences among the treatments, based on the Duncan test ($p < 0.05$, n = 4).

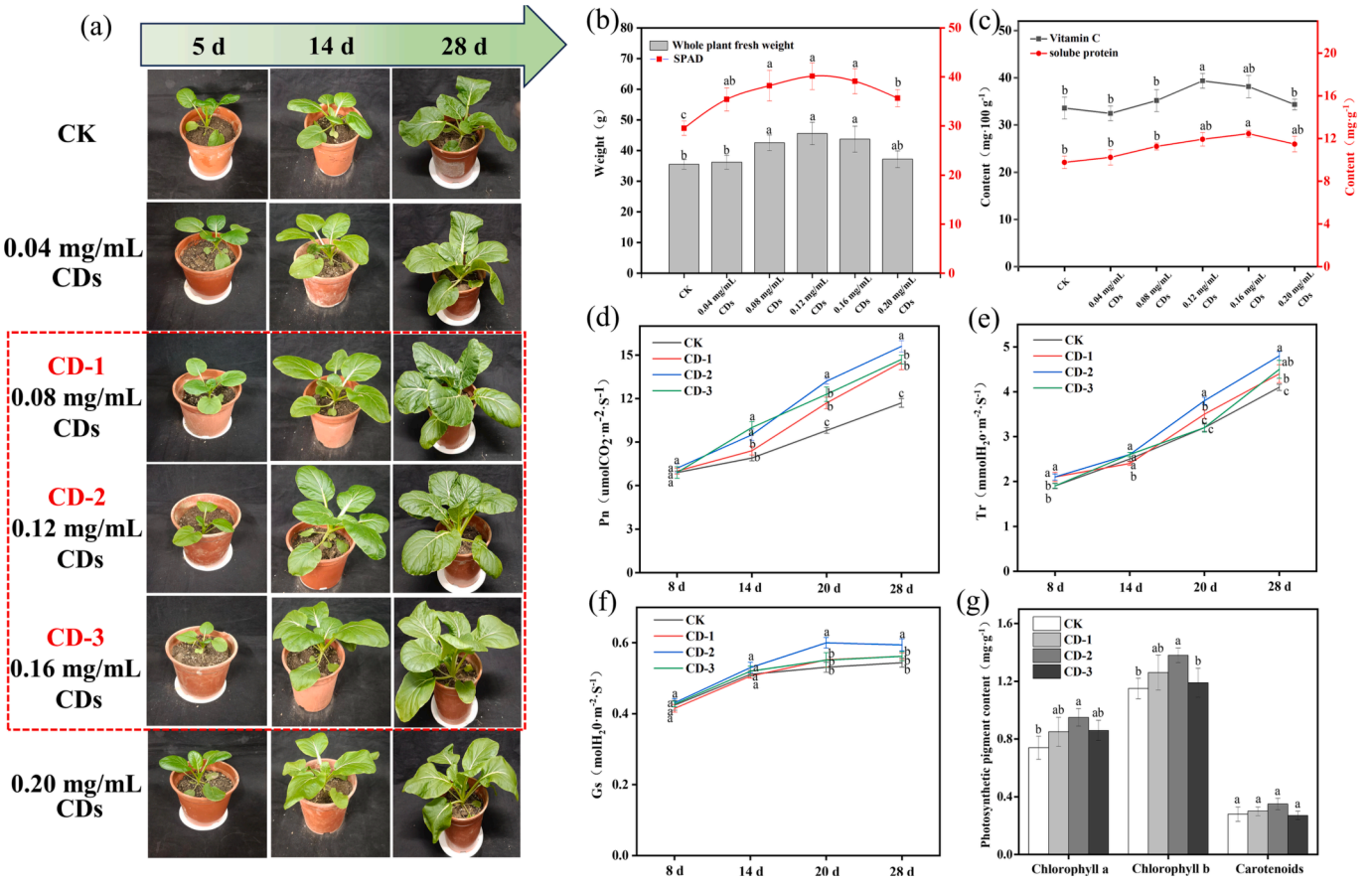

Fig. 4. Effects of different concentrations of CDs on the growth of Choy sum (a). The total fresh mass of Choy sum and leaf SPAD (b). Vitamin C and soluble protein content in leaves (c). The net photosynthetic rate (d), transpiration rate (e), stomatal conductance (f), Photosynthetic pigment content in leaves (g). Different lowercase letters indicate significant differences among the treatments, based on the Duncan test ($p < 0.05$, n = 4).

POP-CDs acting as a light harvester, absorbing ultraviolet light, which is difficult for plant chloroplasts to use, and emitting a specific wavelength of absorbable blue light promoting the synthesis of chlorophyll in Choy sum. Meanwhile, damage to chlorophyll caused by ROS due to light exposure, among other factors, can be alleviated by COS-POP-CDs entering the cell (Wang et al., 2017). This resulted also provides a certain reference value for COS-POP-CDs to delay the senescence of after harvest Choy sum.

3.5. *Flavor compounds of Choy sum*

Not only yield but flavor indicators also decide the economic benefit of Choy sum. Therefore, this study determined the main volatile components in Choy sum leaves after spraying COS-POP-CDs, which can reflect the nutritional and taste senses levels of vegetables (Wei et al., 2021). As shown in Table 1, a total of 50 main volatile compounds were detected in Choy sum leaves treated with different spraying times CDs. The primary compounds were alcohols and esters, with no detection of amines. The alcohols with relatively high abundance were (Z)-3-Hexen-1-ol, 1-Penten-3-ol, 1-Hexanol, and (E)-3-Hexen-1-ol. The esters with the higher relative abundance were (Z)-3-Hexeny-1-ol acetate and Butane-4-isothiocyanate, and there is a certain degree of positive correlation with the times of spraying. Some studies showed that (Z)-3-Hexenyl acetate is a volatile compound that stimulates plant defense systems and participates in plant-plant signaling, while Butane-4-isothiocyanate, a degradation product of glucosinolates, affects the flavor and pungency of crop, it also has antioxidant function (Maurya, Pazouki, & Frost, 2022).

Among the alcohol compounds, T2 treatment had increased the content of 1-Hexanol and 1-Penten-3-ol, 1-Hexanol is a fruity fragrance compound widely present in citrus, berry, violet essential oils, 1-Penten-3-ol is a volatile substance associated with the aroma of strawberry juice. (Z)-3-Hexen-1-ol is produced from 13(S)-hydroperoxy-(9Z,11E)-octadecadienoic acid via the lipoxygenase pathway, and can isomerize into (E)-3-Hexen-1-ol, which plants often release when subjected to biotic and abiotic stress (Cofer, Seidl-Adams, & Tumlinson, 2018). The decreased in the relative abundance of this substance may be related to COS-POP-CDs relieving the stress of Choy sum. Additionally, (Z)-3-Hexen-1-ol is associated with some fresh scents like jasmine (Zhang et al., 2023). Compared with the CK treatment, this study showed that CDs treatment reduced the content of (Z)-3-Hexen-1-ol. CD-2 treatment increased the ratio of ester and aldehyde compounds and reduced the relative content of alcohols. It was worth noting that CDs treatment enhanced the accumulation of isothiocyanates in Choy sum leaves. Isothiocyanates are small molecular compounds produced by the enzymatic degradation of glucosinolates in black mustard and are the main constituents of the pungent odor of Choy sum. Studies have found that isothiocyanates possess natural antimicrobial activity and broad-spectrum bactericidal properties (Plaszkó et al., 2022). Furthermore, they can inhibit the proliferation of tumor cells in vivo through various mechanisms, such as inducing the production of reactive oxygen in tumor cells, causing cell cycle arrest, and promoting tumor cell apoptosis.

3.6. *Effects of COS-POP-CDs on transplanting and after harvest quality of Choy sum*

NBT can react with superoxide anion ($O_2^{\cdot-}$) to generate insoluble blue

Table 1
The relative contents of volatile compounds in choy sum with different treatments.

Group (No.)	Volatile compound	Relative contents (%)		
		CK	T1[a]	T2
Hydrocarbon	3-Ethyl-1,5-octadiene	0.26	0.22	0.16
	2,3-Dimethylpentane	1.22	1.21	0.98
	Toluene	0.54	0.33	/
	2,6,10,14-Tetramethyl-hexadecane	0.24	/	0.03
Alcohols	3-Pentanol	0.26	0.24	0.16
	1-Penten-3-ol	1.08	2.22	2.49
	(Z)-3-Hexen-1-ol	29.2	27.2	25.3
	1-Hexanol	3.89	5.22	6.21
	(E)-3-Hexen-1-ol	3.82	2.17	2.88
	2-Cyclopentaneethanol	0.37	0.38	0.42
	4-Penten-1-ol	0.63	0.69	0.84
	3-Buten-1-ol	0.35	0.32	0.45
	(E)-2-Hexen-1-ol	0.28	0.37	0.42
	2-Ethylhexanol	0.18	0.36	0.44
Carboxylic	Acetic acid	0.44	0.44	0.48
	Aminocyclopropanecarboxylic acid	0.03	0.03	0.02
Esters	Methyl acetate	0.47	0.23	0.08
	Ethyl acetate	0.21	0.27	0.85
	(Z)-2-Penten-1-ol acetate	0.49	0.15	0.34
	(Z)-3-Hexen-1-ol acetate	29.55	26.24	27.12
	(Z)-2-Hexen-1-ol acetate	0.66	0.41	0.44
	Methyl thiocyanate	1.52	3.52	4.28
	Ethyl formate	0.43	0.52	0.88
	(Z)-3-Hexenyl propionate	0.25	0.12	0.18
	1-Butenyl-4-isothiocyanate	0.63	0.88	1.76
	(E)-3-Hexen-1-ol acetate	0.19	0.08	0.06
	3-Cyclohexen-1-ol acetate	0.4	0.62	0.74
	Butane-4-isothiocyanate	2.87	4.44	7.24
	Methyl laurate	0.01	0.01	0.04
	(E)-3-Hexylbutyrate	0.16	0.08	0.52
	2-Methylhexyl butyrate	0.29	0.25	0.04
	(Z)-3-Hexenol-2-methylbutyrate	0.31	0.08	0.02
	(4E)-4-Hexen-1-ol acetate	0.14	0.25	0.09
	Heptyl acetate	0.16	0.21	0.13
	Ethyl laurate	0.08	0.02	/
	3-Butenyl isothiocyanate	0.24	0.08	0.02
Ketone	2,2-Dimethyl-3-heptanone	0.12	0.05	/
	3-Pentanone	0.1	0.15	0.07
	2-(1-butyl-2-nitroallyl) cyclohexanone	0.46	1.21	1.33
	2-Azacyclooctanone	0.34	0.18	0.71
Nitriles	5-Cyano-1-pentene	0.21	0.25	0.52
	Methallyl cyanide	4.77	4.33	3.27
	Butanenitrile,2-methyl-	0.05	0.52	0.12
	$CH_2 = CHCH_2SCH_2CN$	0.05	0.48	0.08
Ethers	Propylene glycol methyl ether	0.15	0.35	0.21
Phenols	Phenol	0.05	0.32	0.12
Aldehydes	3-Hexenal	3.52	5.21	2.14
	(E)-2-Hexenal	0.44	0.15	0.12
	Hexanal	0.25	0.09	0.05
	(E, E)-2,4-Hexadienal	1.21	3.21	1.24

[a] T1 and T2 indicated spraying 0.12 mg/mL COS-POP-CDs once and twice treatment, respectively. "/" indicated not detected.

products, often used for evaluating the content of $O_2^{\cdot-}$ in plant tissue (Tang et al., 2023). Staining results of the leaf tissue showed that compared with the control treatment, CD-1, CD-2, and CD-3 treatments can all reduce the amount of $O_2^{\cdot-}$ in the leaves of Choy sum. It's worth noting that the CD-2 treatment demonstrates better performance in eliminating $O_2^{\cdot-}$in the leaves (Fig. 5A1).

Furthermore, a significant impact on the antioxidant enzyme system of Choy sum has been found through the application of COS-POP-CDs. After 14 d of transplanting, which was 4 d after the first treatment, compared with the CK treatment, the activity of SOD was increased by 40.54 %, POD activity by 77.04 %, and CAT activity by 55.75 %, and the MDA content was reduced 9.86 %. After 28 d of transplanting, which was 8 d after the second spraying treatment, the decline in MDA content in Choy sum leaves became more noticeable, reaching 18.97 %. The increased activity of SOD enzyme in the leaves was further elevated, with a rise reaching up to 63.24 %, however, the increase in POD and CAT enzyme activities didn't significantly much with two times of CD-2 application (Fig. 5A2–A5).

In addition, the expressions of three antioxidant enzyme genes (*CsMn-SOD*, *Cs-POD*, *Cs-CAT*) were shown in (Fig. 5A6-A8), after 14 and 24 d transplanting of Choy sum, The expressions of *CsMn-SOD*, *Cs-POD*, and *Cs-CAT* increased with the growth of Choy sum. Compared with the CK treatment, the expression levels of SOD, POD, CAT related genes were found to be upregulated by 3.41–4.13, 2.69–4.08, and 1.61–2.25 fold, respectively. Compared with CD-1 and CD-3 treatments, spraying CD-2 twice could significantly increase the expression of SOD and POD related genes in Choy sum, but could not significantly enhance the expression of its CAT gene. After 28 d of transplanting Choy sum, the expression of SOD and POD related genes gradually declined, and the differences treatments were not significant between CD-1 and CD-3 ($p < 0.05$). The above results exhibited that COS-POP-CDs could maintain the cellular antioxidant system, protect cell membrane structures, mitigate oxidative damage brought about by ROS, and suitable concentrations of COS-POP-CDs can significantly enhance the gene expression of the antioxidant enzyme system.

After harvesting, significant slowing of the wilting of Choy sum leaves was observed with once foliar spray of COS-POP-CDs. The leaf slice analysis results demonstrated that CD-1, CD-2, and CD-3 treatments all improved the number of chloroplasts per unit area in the leaves. Among these, CD-2 treatment chloroplasts were brighter green (Fig. 5B1). This could be because in the early stage after harvest, cell activity is high, and the CDs can still promote the synthesis of chlorophyll in Choy sum leaves (Kuang et al., 2023). As shown in Fig. 5B2, the treatment with CDs reduced the water loss of after harvest Choy sum. After 6, 8, and 10 d of natural storage, the water loss rates for the CK treatment of Choy sum were 8.1 %, 9.0 %, and 10.3 %, respectively. Compared with the CK treatment, the Choy sum treated with CD-2, the water loss rates were significantly lower at 6.2 %, 7.0 %, and 8.1 %, respectively ($p < 0.05$). After 4, 6, 8, and 10 d of storage, analysis of the nutritional quality of Choy sum found that the Vitamin C content in the Choy sum treated with CD-2 was 23.41 %, 30.43 %, 43.32 %, and 32.56 % higher than the CK treatment, respectively, all reaching significant differences ($p < 0.05$) (Fig. 5B3). After 4, 6, and 8 d of storage, compared with the CK treatment. the soluble protein in Choy sum treated with CD-2 increased by 15.12 %, 22.63 %, and 20.04 %. Interestingly, as the storage time increased, the difference in soluble protein content gradually narrowed (Fig. 5B4). The content of soluble solids in the Choy sum leaves was observed to first increase and then decrease. After 4, 6, and 8 d of storage, the soluble solids content of the COS-POP-CDs treatment was 6.67 %, 7.38 %, and 21.42 % higher than that of the control, respectively (Fig. 5B5).

During the selling process, Choy sum is inevitably contaminated by bacteria in nature (Palumbo et al., 2022), so we evaluated the effect of spraying different concentrations of COS-POP-CDs on the number of bacteria on the surface of Choy sum. The results showed that CD-2 treatment could significantly reduce the number of bacteria on the surface of Choy sum, but the difference between CDs treatments was small, which may be related to the small difference in the concentration of sprayed COS-POP-CDs (Fig. 5B6). Previous studies have shown that the expression of antioxidant enzyme system-related genes can be increased by spraying COS-POP-CDs before harvesting Choy sum. Therefore, after harvest spraying with once COS-POP-CDs treatment, the changes in MDA and the antioxidants SOD, POD, and CAT in the leaves at different storage times were measured. The results showed that as the storage time extended, the MDA content gradually increased. After 2 d of storage, there was no significant difference between the treatments. When stored for 4, 6, and 8 d, the MDA in Choy sum treated with CD-2 was 13.33 %, 18.63 %, and 14.25 % lower than that of the CK treatment,

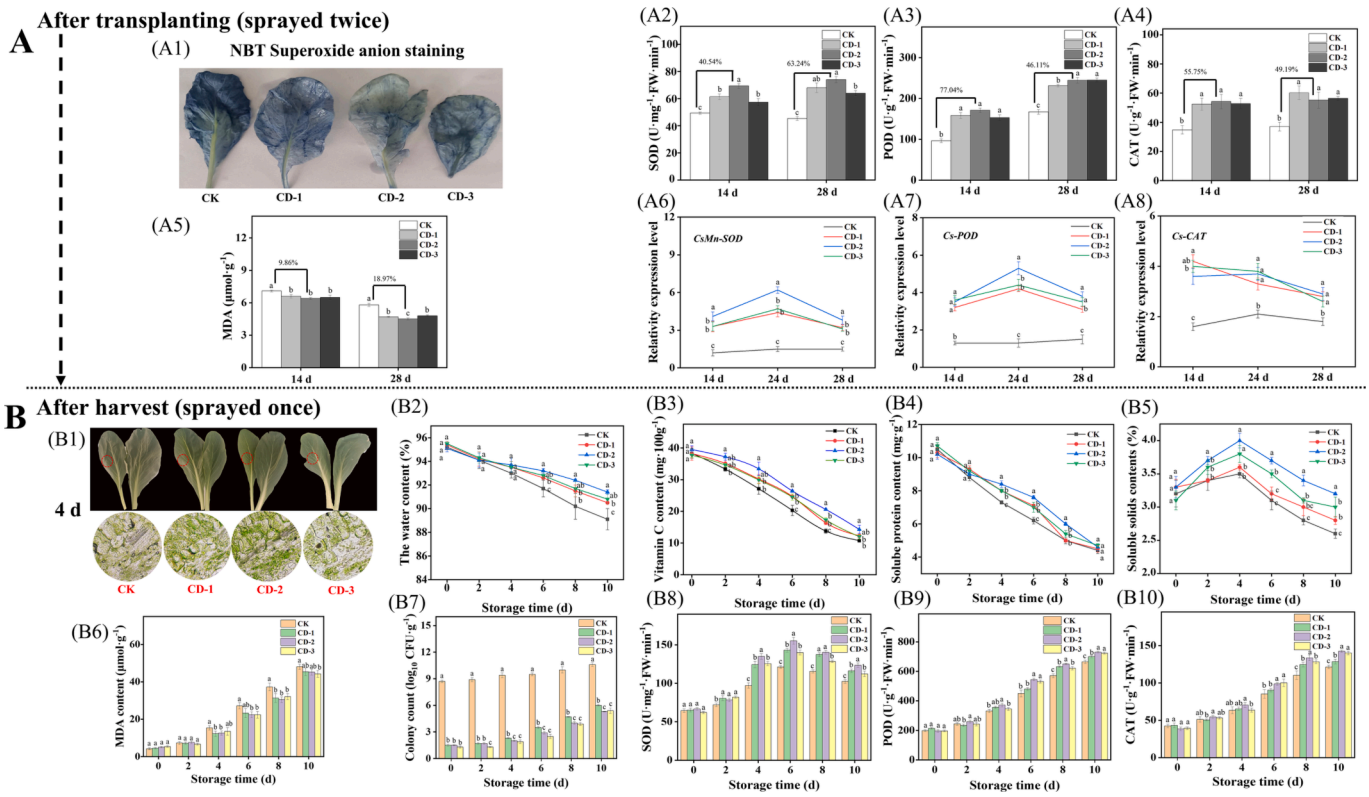

Fig. 5. After transplanting (Fig. 5A): NBT Choy sum leaf tissue staining (A1). Different concentrations of COS-POPs-CDs improve the leaf antioxidant enzymes and reduce MDA content (A2, A3, A4, A5). The expression of antioxidant enzyme-related genes (A6, A7, A8). After harvest (Fig. 5B): Appearance of Choy sum after harvest 4 d (B1). Changes of water content, vitamin C, soluble protein, soluble solid content, and colony count in after harvest Choy sum leaves (B2, B3, B4, B5, B6). Effect of Different concentrations of COS-POPs-CDs on leaf antioxidant enzymes and MDA content (B7, B8, B9, B10). Different lowercase letters indicate significant differences among the treatments, based on the Duncan test ($p < 0.05$, n = 4).

respectively, reaching a significant level ($p < 0.05$) (Fig. 5B7). However, the difference between treatments gradually narrowed after 10 d of storage. As shown in Fig. 5B8, B9, B10, after harvest spraying COS-POP-CDs once can significantly increase the content of antioxidant enzymes SOD, POD, and CAT in Choy sum leaves in the later stage of storage. Compared with the CK treatment, during 4–10 d of storage, the activities of SOD (30.76–57.91 %), POD (23.12–44.95 %) and CAT (36.82–63.56 %) enzymes increased in the leaves, respectively, throughout the treatment period for CD-2 treatment, but CD-1, CD-2, CD-3 treatments were small in antioxidant enzyme activities.

4. Conclusions

Our study synthesized a composite material COS-POP-CDs successfully through high-temperature at Maillard reaction cross-links COS and POP. Compared with COS-CDs and POP-CDs, the novel carbon dots had smaller size of 3.2 ± 1.1 nm. Meanwhile, their fluorescence characteristics were found to overlap significantly with the blue-violet wavelength absorption region of chloroplasts. Moreover, COS-POP-CDs exhibited strong in vitro antioxidant and antibacterial activities. Foliar application of 0.12 mg/mL COS-POP-CDs twice could rapidly induce the activation of the leaf antioxidant system, and also enhanced the photosynthesis and the yield of Choy sum. Worthy, COS-POP-CDs enhanced the contents of spicy and strawberry fragrance flavors of Choy sum. After harvest, a single application of 0.12 mg/mL COS-POP-CDs could scavenge ROS, delay the breakdown of chloroplasts, Concurrently, it elevated the antioxidant enzyme activity in Choy sum and maintained the nutritional content of the plant. In summary, the study presented COS-POP-CDs as an innovative material, which can extend the shelf life of leaf vegetable, thus improving economic efficiency.

CRediT authorship contribution statement

Bosi Lu: Investigation, Writing – original draft. **Xiaojuan Chen:** Investigation. **Xin OuYang:** Investigation. **Zhiming Li:** Resources. **Xujian Yang:** Resources. **Zaid Khan:** Resources. **Songpo Duan:** Resources, Validation. **Hong Shen:** Formal analysis, Project administration, Supervision.

Declaration of Competing Interest

The authors declare that they have no known competing financial interests or personal relationships that could have appeared to influence the work reported in this paper.

Data availability

The data that has been used is confidential.

Acknowledgement

This work was supported by the Science and Technology Planning Project of Guangzhou (No.202206010064), Guangdong Province General and High Efficiency Key Field Research Project (2020ZDZX1002) and the National Key Research and Development Program of China (2016YFD0200405-5).

Appendix A. Supplementary data

Supplementary data to this article can be found online at https://doi.org/10.1016/j.fochx.2023.100963.

References

Ailincai, D., Rosca, I., Morariu, S., Mititelu-Tartau, L., & Marin, L. (2022). Iminoboronate-chitooligosaccharides hydrogels with strong antimicrobial activity for biomedical applications. *Carbohydrate Polymers, 276*, Article 118727. https://doi.org/10.1016/j.carbpol.2019.03.063

Chen, F., Huang, G., Yang, Z., & Hou, Y. (2019). Antioxidant activity of Momordica charantia polysaccharide and its derivatives. *International journal of biological macromolecules, 138*, 673–680. https://doi.org/10.1016/j.ijbiomac.2019.07.129

Cofer, T. M., Seidl-Adams, I., & Tumlinson, J. H. (2018). From acetoin to (Z)-3-hexen-1-ol: the diversity of volatile organic compounds that induce plant responses. *Journal of agricultural and food chemistry, 66*(43), 11197–11208. https://doi.org/10.1021/acs.jafc.8b03010

Cui, D. D., Yang, J., Lu, B. S., Deng, L. S., & Shen, H. (2022). Extraction and characterization of chitin from Oratosquilla oratoria shell waste and its application in *Brassica campestris* L. ssp. *International Journal of Biological Macromolecules, 198*, 204–213. https://doi.org/10.1016/j.ijbiomac.2021.12.173

Cui, M., Ren, S., Zhao, H., Wang, L., & Xue, Q. (2018). Novel nitrogen doped carbon dots for corrosion inhibition of carbon steel in 1 M HCl solution. *Applied Surface Science, 443*, 145–156. https://doi.org/10.1016/j.apsusc.2018.02.255

Đorđević, L., Arcudi, F., Cacioppo, M., & Prato, M. (2022). A multifunctional chemical toolbox to engineer carbon dots for biomedical and energy applications. *Nature Nanotechnology, 17*(2), 112–130. https://doi.org/10.1038/s41565-021-01051-7

Ezati, P., Rhim, J. W., Molaei, R., Priyadarshi, R., Roy, S., Min, S., Han, S., et al. (2022). Preparation and characterization of B, S, and N-doped glucose carbon dots: Antibacterial, antifungal, and antioxidant activity. *Sustainable Materials and Technologies, 32*, Article e00397. https://doi.org/10.1016/j.susmat.2022.e00397

Farooq, M. A., Hannan, F., Islam, F., Ayyaz, A., Zhang, N., Chen, W., et al. (2022). The potential of nanomaterials for sustainable modern agriculture: Present findings and future perspectives. *Environmental Science: Nano, 9*(6), 1926–1951. https://doi.org/10.1039/D1EN01124C

Fu, B., Liu, Q., Liu, M., Chen, X., Lin, H., Zheng, Z., et al. (2022). Carbon dots enhanced gelatin/chitosan bio-nanocomposite packaging film for perishable foods. *Chinese Chemical Letters, 33*(10), 4577–4582. https://doi.org/10.1016/j.cclet.2022.03.048

Gao, M., Chang, J., Wang, Z., Zhang, H., & Wang, T. (2023). Advances in transport and toxicity of nanoparticles in plants. *Journal of Nanobiotechnology, 21*(1), 75. https://doi.org/10.1186/s12951-023-01830-5

Guo, J., Lu, Y., Xie, A. Q., Li, G., Liang, Z. B., Wang, C. F., & Chen, S. (2022). Yellow-emissive carbon dots with high solid-state photoluminescence. *Advanced Functional Materials, 32*(20), Article 2110393. https://doi.org/10.1002/adfm.202110393

He, J. H., Cheng, Y. Y., Zhang, Q. Q., Liu, H., & Huang, C. Z. (2020). Carbon dots-based fluorescence resonance energy transfer for the prostate specific antigen (PSA) with high sensitivity. *Talanta, 219*, Article 121276. https://doi.org/10.1016/j.talanta.2020.121276

Jang, M. H., Song, S. H., Ha, H. D., Seo, T. S., Jeon, S., & Cho, Y. H. (2017). Origin of extraordinary luminescence shift in graphene quantum dots with varying excitation energy: An experimental evidence of localized sp^2 carbon subdomain. *Carbon, 118*, 524–530. https://doi.org/10.1016/j.carbon.2017.03.060

Jia, X., Li, J., & Wang, E. (2012). One-pot green synthesis of optically pH-sensitive carbon dots with upconversion luminescence. *Nanoscale, 4*(18), 5572–5575. https://doi.org/10.1039/C2NR31319G

Ke, Y., Ding, B., Zhang, M., Dong, T., Fu, Y., Lv, Q., et al. (2022). Study on inhibitory activity and mechanism of chitosan oligosaccharides on Aspergillus Flavus and Aspergillus Fumigatus. *Carbohydrate Polymers, 275*, Article 118673. https://doi.org/10.1016/j.carbpol.2021.118673

Khalid, M. F., Huda, S., Yong, M., Li, L., Li, L., Chen, Z. H., et al. (2023). Alleviation of drought and salt stress in vegetables: crop responses and mitigation strategies. *Plant Growth Regulation, 99*(2), 177–194. https://doi.org/10.1007/s10725-022-00905-x

Koutamehr, M. E., Moradi, M., Tajik, H., Molaei, R., Heshmati, M. K., & Alizadeh, A. (2023). Sour whey-derived carbon dots; synthesis, characterization, antioxidant activity and antimicrobial performance on foodborne pathogens. *LWT, 114978*. https://doi.org/10.1016/j.lwt.2023.114978

Kuang, L., Kang, Y., Wang, H., Huang, R., Lei, B., Zhong, M., et al. (2023). The roles of *Salvia miltiorrhiza*-derived carbon dots involving in maintaining quality by delaying senescence of postharvest flowering Chinese cabbage. *Food Chemistry, 404*, Article 134704. https://doi.org/10.1016/j.foodchem.2022.134704

Laurentin, A., & Edwards, C. A. (2003). A microtiter modification of the anthrone-sulfuric acid colorimetric assay for glucose-based carbohydrates. *Analytical Biochem., 315*, 143–145. https://doi.org/10.1016/S0003-2697(02)00704-2

Leng, L., Liu, R., Xu, S., Mohamed, B. A., Yang, Z., Hu, Y., et al. (2022). An overview of sulfur-functional groups in biochar from pyrolysis of biomass. *Journal of Environmental Chemical Engineering, 10*(2), Article 107185. https://doi.org/10.1016/j.jece.2022.107185

Li, W., Wu, S., Zhang, H., Zhang, X., Zhuang, J., Hu, C., Wang, X., et al. (2018). Enhanced biological photosynthetic efficiency using light-harvesting engineering with dual-emissive carbon dots. *Advanced Functional Materials, 28*(44), Article 1804004. https://doi.org/10.1002/adfm.201804004

Li, W., Zhang, H., Zheng, Y., Chen, S., Liu, Y., Zhuang, J., et al. (2017). Multifunctional carbon dots for highly luminescent orange-emissive cellulose based composite phosphor construction and plant tissue imaging. *Nanoscale, 9*(35), 12976–12983. https://doi.org/10.1039/C7NR03217J

Li, Z., Duan, S., Lu, B., Yang, C., Ding, H., & Shen, H. (2023). Spraying alginate oligosaccharide improves photosynthetic performance and sugar accumulation in citrus by regulating antioxidant system and related gene expression. *Frontiers in Plant Science, 13*, Article 1108848. https://doi.org/10.3389/fpls.2022.1108848

Liu, X., Hou, W., Huang, Y., Zhao, H., Song, Z., & Huang, Y. (2022). Facile and green synthesis of carbon nanopinnacles for the removal of chlortetracycline: performance, mechanism and biotoxicity. *Chemical Engineering Journal, 433*, Article 133822. https://doi.org/10.1016/j.cej.2021.133822

Lucarini, E., Micheli, L., Di Cesare Mannelli, L., & Ghelardini, C. (2022). Naturally occurring glucosinolates and isothiocyanates as a weapon against chronic pain: potentials and limits. *Phytochemistry Reviews, 21*(2), 647–665. https://doi.org/10.1007/s11101-022-09809-0

Mao, L., Wang, X., Guo, Y., Yao, L., Xue, X., Wang, H. X., et al. (2019). A synergistic approach to enhance the photoelectrochemical performance of carbon dots for molecular imprinting sensors. *Nanoscale, 11*(16), 7885–7892. https://doi.org/10.1039/C9NR01675A

Maurya, A. K., Pazouki, L., & Frost, C. J. (2022). Priming seeds with indole and (Z)-3-hexenyl acetate enhances resistance against herbivores and stimulates growth. *Journal of Chemical Ecology, 48*(4), 441–454. https://doi.org/10.1007/s10886-022-01359-1

Milanović, Ž., Dimić, D., Antonijević, M., Žižić, M., Milenković, D., Avdović, E., et al. (2023). Influence of acid-base equilibria on the rate of the chemical reaction in the advanced oxidation processes: coumarin derivatives and hydroxyl radical. *Chemical Engineering Journal, 453*, Article 139648. https://doi.org/10.1016/j.cej.2022.139648

Muthamma, K., Sunil, D., & Shetty, P. (2021). Carbon dots as emerging luminophores in security inks for anti-counterfeit applications-an up-to-date review. *Applied Materials Today, 23*, Article 101050. https://doi.org/10.1016/j.apmt.2021.101050

Palumbo, M., Attolico, G., Capozzi, V., Cozzolino, R., Corvino, A., de Chiara, M. L. V., et al. (2022). Emerging postharvest technologies to enhance the shelf-life of fruit and vegetables: an overview. *Foods, 11*(23), 3925. https://doi.org/10.3390/foods11233925

Plaszkó, T., Szűcs, Z., Vasas, G., & Gonda, S. (2022). Interactions of fungi with non-isothiocyanate products of the plant glucosinolate pathway: A review on product formation, antifungal activity, mode of action and biotransformation. *Phytochemistry, 200*, Article 113245. https://doi.org/10.1016/j.phytochem.2022.113245

Samynathan, R., Venkidasamy, B., Shanmugam, A., Khaled, J. M., Chung, I. M., & Thiruvengadam, M. (2023). Investigating the impact of tea mosquito bug on the phytochemical profile and quality of Indian tea cultivars using HPLC and LC-MS-based metabolic profiling. *Industrial Crops and Products, 204*, Article 117278. https://doi.org/10.1016/j.indcrop.2023.117278

Shaik, M. A. S., Samanta, D., Shaw, M., Mondal, I., Basu, R., & Pathak, A. (2022). Fluorescent N, S co-doped carbon dots for tartrazine sensing and mechanistic perception of their radical scavenging activity. *Sensors and Actuators Reports, 4*, Article 100127. https://doi.org/10.1016/j.snr.2022.100127

Shimakawa, G. (2023). Electron transport in cyanobacterial thylakoid membranes: are cyanobacteria simple models for photosynthetic organisms? *Journal of Experimental Botany, erad118*. https://doi.org/10.1093/jxb/erad118

Sk, M. P., Jaiswal, A., Paul, A., Ghosh, S. S., & Chattopadhyay, A. (2012). Presence of amorphous carbon nanoparticles in food caramels. *Scientific reports, 2*(1), 383. https://doi.org/10.1038/srep00383

Slavin, J. L., & Lloyd, B. (2012). Health benefits of fruits and vegetables. *Advances in nutrition, 3*(4), 506–516. https://doi.org/10.3945/an.112.002154

Tang, Y., Zhang, J., Wang, L., Wang, H., Long, H., Yang, L., et al. (2023). Water deficit aggravated the inhibition of photosynthetic performance of maize under mercury stress but is alleviated by brassinosteroids. *Journal of Hazardous Materials, 443*, Article 130365. https://doi.org/10.1016/j.jhazmat.2022.130365

Wang, C., Yang, H., Chen, F., Yue, L., Wang, Z., & Xing, B. (2021). Nitrogen-doped carbon dots increased light conversion and electron supply to improve the corn photosystem and yield. *Environmental Science & Technology, 55*(18), 12317–12325. https://doi.org/10.1021/acs.est.1c01876

Wang, M., Gao, L., Dong, S., Sun, Y., Shen, Q., & Guo, S. (2017). Role of silicon on plant–pathogen interactions. *Frontiers in Plant Science, 8*, 701. https://doi.org/10.3389/fpls.2017.00701

Wang, Y., Li, S., Liu, L., Lv, F., & Wang, S. (2017). Conjugated polymer nanoparticles to augment photosynthesis of chloroplasts. *Angewandte Chemie International Edition, 56*(19), 5308–5311. https://doi.org/10.1002/anie.201702376

Wei, S., Xiao, X., Wei, L., Li, L., Li, G., Liu, F., et al. (2021). Development and comprehensive HS-SPME/GC–MS analysis optimization, comparison, and evaluation of different cabbage cultivars (Brassica oleracea L. var. capitata L.) volatile components. *Food Chemistry, 340*, Article 128166. https://doi.org/10.1016/j.foodchem.2020.128166

Wei, W., Xu, C., Wu, L., Wang, J., Ren, J., & Qu, X. (2014). Non-enzymatic-browning-reaction: A versatile route for production of nitrogen-doped carbon dots with tunable multicolor luminescent display. *Scientific reports, 4*(1), 1–7. https://doi.org/10.1038/srep03564

Xu, Y., Zhang, J., Pan, T., Ren, F., Luo, H., & Zhang, H. (2022). Synthesis, characterization and effect of alkyl chain unsaturation on the antioxidant activities of chlorogenic acid derivatives. *LWT, 162*, Article 113325. https://doi.org/10.1016/j.lwt.2022.113325

Yu, G., & Klionsky, D. J. (2022). A "short-cut" response of autophagy to oxidative stress: Oxygen-dependent activity of a lysine demethylase guides the activity of ULK1 during hypoxia. *Autophagy, 18*(8), 1749–1751. https://doi.org/10.1080/15548627.2022.2089957

Zhang, C., Zhou, C., Tian, C., Xu, K., Lai, Z., Lin, Y., et al. (2023). Volatilomics analysis of jasmine tea during multiple rounds of scenting processes. *Foods, 12*(4), 812. https://doi.org/10.3390/foods12040812

Zhang, Y., Wang, Y., Feng, X., Zhang, F., Yang, Y., & Liu, X. (2016). Effect of reaction temperature on structure and fluorescence properties of nitrogen-doped carbon dots.

Applied Surface Science, 387, 1236–1246. https://doi.org/10.1016/j.apsusc.2016.07.048